Institute of Paper Science and Technology
Atlanta, Georgia

IPST Technical Paper Series Number 924

Aggregation Behavior of Antimony (V) Porphyrins in Polyfluorinated Surfactant/Clay Hybrid Microstructures

L. Lucia, T Yui, R. Sasai, T. Shinsuke, T. Katsuhiko, D.G. Whitten, and H. Inoue

January 2002

Submitted to
The Journal of Physical Chemistry
Part B

INSTITUTE OF PAPER SCIENCE AND TECHNOLOGY
PURPOSE AND MISSIONS

The Institute of Paper Science and Technology is an independent graduate school, research organization, and information center for science and technology mainly concerned with manufacture and uses of pulp, paper, paperboard, and other forest products and byproducts. Established in 1929 as the Institute of Paper Chemistry, the Institute provides research and information services to the wood, fiber, and allied industries in a unique partnership between education and business. The Institute is supported by 51 member companies. The purpose of the Institute is fulfilled through four missions, which are:

- to provide a multidisciplinary graduate education to students who advance the science and technology of the industry and who rise into leadership positions within the industry;
- to conduct and foster research that creates knowledge to satisfy the technological needs of the industry;
- to provide the information, expertise, and interactive learning that enable customers to improve job knowledge and business performance;
- to aggressively seek out technological opportunities and facilitate the transfer and implementation of those technologies in collaboration with industry partners.

ACCREDITATION

The Institute of Paper Science and Technology is accredited by the Commission on Colleges of the Southern Association of Colleges and Schools to award the Master of Science and Doctor of Philosophy degrees.

NOTICE AND DISCLAIMER

The Institute of Paper Science and Technology (IPST) has provided a high standard of professional service and has put forth its best efforts within the time and funds available for this project. The information and conclusions are advisory and are intended only for internal use by any company who may receive this report. Each company must decide for itself the best approach to solving any problems it may have and how, or whether, this reported information should be considered in its approach.

IPST does not recommend particular products, procedures, materials, or service. These are included only in the interest of completeness within a laboratory context and budgetary constraint. Actual products, materials, and services used may differ and are peculiar to the operations of each company.

In no event shall IPST or its employees and agents have any obligation or liability for damages including, but not limited to, consequential damages arising out of or in connection with any company's use of or inability to use the reported information. IPST provides no warranty or guaranty of results.

Aggregation Behavior of Antimony (V) Porphyrins in Polyfluorinated Surfactant/Clay Hybrid Microstructures

Lucian A. Lucia,[a,†] Tatsuto Yui,[b] Ryo Sasai,[c] Takagi Shinsuke,[b] Takagi Katsuhiko,[c] David G. Whitten,[a,‡] Haruo Inoue [*,b,d]

(a) Department of Chemistry, University of Rochester, Rochester, New York 14627

(b) Department of Applied Chemistry, Graduate Course of Engineering, Tokyo Metropolitan University, 1-1 Minami-ohsawa, Hachiohji-city, Tokyo 192-0397, Japan

(c) Department of Crystalline Materials Science, Graduate School of Engineering, Nagoya University, Furo-cho, Chikusa-ku, 464-8603, Japan

(d) CREST (Japan Science and Technology)

† Current address: Institute of Paper Science and Technology, Georgia Institute of Technology, 500 10th Street N.W., Atlanta, GA 30318-5794.

‡ Current address: Chemical Science and Technology Division, Los Alamos National Laboratory, Los Alamos, New Mexico 87545.

Abstract

The polyfluorinated surfactant ($C_nF_{2n+1}CONH(CH_2)_2N^+(CH_3)_2C_{16}H_{33}$ Br^-; designated as CnF-S, where n=1-3)/clay hybrid microstructures has been shown to generate polyfluorinated microcavities in the clay interlayers with known molecular dimensions (Yui et al., *Langmuir*, in press). The aggregation behavior of a water-soluble porphyrin (*tetra*-(4-sulfonatophenyl)porphyrinatoantimony (V); Sb(V)TSPP) that cointercalated (with a surfactant) in the polyfluorinated microcavity was investigated. One of the key findings in this study was that the absorption spectra of Sb(V)TSPP molecules that were intercalated in C3F-S

polyfluorinated surfactant/clay hybrid microstructures were drastically changed upon dispersion in benzene. The monomer Soret absorption band of Sb(V)TSPP (422 nm) was observed to split into both a longer (438-nm) and a shorter (388-nm) wavelength component. These coincident spectral changes were dependent on the adsorbed amount of Sb(V)TSPP and were adequately fit by computer simulation curve fitting that was based on the assumption of dimer formation. The absorption and emission measurements as supported by the simulated fits suggest that two types of dimers (J and H dimers) were formed in the polyfluorinated surfactant/clay hybrid interlayers. It was also found that when the adsorbed amount of surfactant molecules was observed to decrease, i.e., when the volume of the polyfluorinated microcavity in the interlayer increased, then the dimerization of Sb(V)TSPP was enhanced. In the case of C2F-S and C1F-S polyfluorinated/clay hybrid compounds, similar spectral behavior arising from dimerization was observed. In contrast, in the case of the hydrocarbon analogs (C3H-S) and cetyltrimethylammonium bromide (CTAB)/clay hybrid compounds, the absorption and emission arising from Sb(V)TSPP indicated that it essentially retained its monomer character. Small-angle x-ray scattering experiments revealed that the clearance space (distance between the layers) for the hybrid compounds in benzene increased compared to that of the solid hybrid compounds. This result indicates a penetration of the benzene molecules into the hybrid layers. Based on the latter results, it is proposed that the aggregation mechanism of Sb(V)TSPP in polyfluorinated surfactant/clay hybrid compounds obeys the following sequence: (1) formation of a polyfluorinated environment of interlayers that have very weak intermolecular interactions among the surfactant molecules, (2) upon penetration of the benzene solvent molecules, swelling of the hybrid compounds and solvation of Sb(V)TSPP into the interlayers, (3) expulsion of Sb(V)TSPP molecules from the polyfluorinated assemblies into the interlayer space, and (4) migration of Sb(V)TSPP molecules to microcavities with concomitant dimer (H and J) formation.

Introduction

Clay minerals possess a layered structure that is characterized by a physical stacking of the alumino silicate sheets.[1-4] Various molecular entities can be reversibly inserted into the layered space (viz., by an intercalation process) through general ion exchange phenomena. This clay layer can self-adjust to accommodate guest species through expansion of interlayer distances. It is well known, for example, that intercalated surfactant-type molecules can form molecular assemblies in which the interlayer space allows a regular distribution of the guest molecules based on intermolecular interactions.[5-9] Thus, the interlayer space can be "functionalized" or chemically tuned by the judicious choice or inclusion of specific functional compounds. This concept is very interesting and powerful since it can expedite the successful intercalation of a third component into a surface-modified clay layer with the formal initiation of chemical reactions. Intercalation of alkylammonium cation-type surfactants, for example, has been well examined from both an industrial and a basic science perspective.[10-17]

Polyfluorinated organic surfactants are a unique class of surfactants that have been the subject of research attention recently.[18-20] Their very weak intermolecular interactions with other molecules can be exploited for various applications. For example, an organic fluorinated compound that behaves as a solvent is expected to relatively enhance solute-solute intermolecular interactions, since solvent(fluorinated compound)-solute interactions are known to be minimized in fluorinated environments.[21] Exploration of chemical reactions in polyfluorinated environments has remained attractive, yet there has been little chance to explore perfluorinated compounds as solvents due to their solubility limits. One of the most promising approaches to solve this issue would be the formation of polyfluorinated solvent environments under molecular architectures such as micelles, reversed micelles, and vesicles.

Thus, in light of the above information, we have synthesized ammonium cation-type polyfluorinated surfactants (CnF-S, where n=1-3, see Scheme) in which they have been found to form micelles with unique fluorinated microenvironments at clay interfaces.[22] Additionally, we have determined that these polyfluorinated surfactants intercalate into the clay layers.[23-25] It was

found that the polyfluorinated surfactants easily intercalated into the clay interlayer spaces of sodium saponite (Sumecton SA, used as a cation-exchange-type clay) to form rigidly packed bilayer structures. The C3F-S polyfluorinated surfactants exhibit intercalation that is 440% of the cation exchange capacity (CEC) of the saturated adsorption limit of the clay. Remarkably, the clay clearance space (distance between layers) maintains a constant value in the bilayer structures at intercalation levels from 100 to 440% CEC. These results indicate that the polyfluorinated surfactant/clay hybrid compounds have the molecular dimensions of a polyfluorinated microcavity that behaves as if it has an absorbed amount of the surfactants equivalent to 100-300% of the CEC. To clarify the molecular representation of the packing phenomenon, a schematic illustration of the polyfluorinated surfactant (C3F-S)/clay hybrid compounds under various adsorbed amounts of C3F-S is shown in Figure 1.[23]

Scheme. Molecular Formula of Surfactants and Sb(V)TSPP

Figure 1. Schematic structure of C3F-S/clay hybrid.

One of the most noteworthy findings in this study is the photophysics and potential photochemistry that is accessible in such polyfluorinated microcavities. The present work describes the application of these cation-exchangeable-type clays for the unique intercalation of metalloporphyrin molecules. We have chosen to study the photophysics and photochemistry of metalloporphyrins since they have been the subject of extensive past research efforts.[26-29] We have therefore initiated a novel investigation of the intercalation behavior of metalloporphyrins in polyfluorinated surfactant/clay hybrid compounds.[25] The *tetra*-(4-sulfonatophenyl)porphyrinatotin(IV) (Sn(IV)TSPP) has been shown to form an aggregate in the interlayers of polyfluorinated surfactant/clay hybrid compounds. The porphyrin aggregates have also received significant attention mainly because of their photochemical and technologically appealing properties.[30-36]

In this investigation, we explored the intercalation and aggregation behavior of *tetra*-(4-sulfonatophenyl)porphyrinatoantimony(V) (Sb(V)TSPP) in sodium saponite clay layers. We also investigated and report a proposed aggregation mechanism of these porphyrins in the polyfluorinated surfactant/clay hybrid environments.

Experimental Section

Materials

The synthesis of polyfluorinated surfactants (CnF-S) and their hydrocarbon analogs (C3H-S) has been reported elsewhere.[22] The subscript *n* denotes the number of carbons in the acyl group, *F* denotes a polyfluorinated surfactant, *H* denotes a hydrocarbon analog, and *S* illustrates a surfactant-type single long alkyl chain. Cetyltrimethylammonium bromide (CTAB; WAKO Pure Chemical Ind. Co.) was recrystallized from acetone.

The *tetra*-(4-sulfonatophenyl)porphyrinatoantimony (V) (Sb(V)TSPP) was synthesized according to the following procedures: SbCl5 (12 mL) was added dropwise to *meso-tetra*-(4-sulfonatophenyl)-21H, 23H-porphyrin dihydrochloride (Porphyrin Product, Inc.) in dry pyridine (1 L), and the reaction mixture was stirred for 9 hours while refluxing under nitrogen atmosphere to form Sb(V)TSPP. Water (100 mL) was added to the reaction mixture and the resultant white precipitate was removed by filtration. The crude Sb(V)TSPP was purified by reprecipitation from acetonitrile, gel filtration (LH-20, eluent; H_2O), and column chromatography (SiO_2, eluent; acetonitrile : H_2O = 4 : 1). Structures of the CnF-S and C3H-S surfactants and Sb(V)TSPP are shown in the provided Scheme.

Cation-exchangeable clays were used in the present work. Sumecton SA is a type of sodium saponite synthesized via a hydrothermal reaction. They have good transparency in the visible region due to the absence of any impurities. The chemical and physical characteristics of Sumecton SA are as follows[37, 38] : the composition is $[(Si_{7.20}\ Al_{0.80})\ (Mg_{5.97}\ Al_{0.03})\ O_{20}\ (OH)_4]^{-0.77}$ $(Na_{0.49}\ Mg_{0.14})^{+0.77}$; the surface area is 750 $m^2\ g^{-1}$; and the cation exchange capacity (CEC) is 0.997 meq g^{-1}.

Deionized water (conductivity < 0.1 mS cm^{-1}) was used as a solvent for intercalation reactions. Benzene (Kanto; spectroscopic grade) was used for all spectroscopic studies.

Sample preparation

The synthesis of surfactant/clay hybrid compounds and cointercalation of Sb(V)TSPP were carried out according to the following procedure:[23-25] in a typical example, 60 mL of aqueous surfactant solution (5 mm) and 4 mL of aqueous Sb(V)TSPP solution (7.9 ′ 10^{-5} m) were added to 10 mL of clay dispersion (10 g L^{-1}). Under these conditions, the loading levels of surfactant and Sb(V)TSPP were 300% and 0.2%, respectively, with respect to the CEC of the clay. Control of the surfactant and Sb(V)TSPP loading levels affected the levels of the adsorbed surfactant and Sb(V)TSPP. An aqueous mixture of Sb(V)TSPP/surfactant/clay was stirred at 60-70°C for 3 hours. The precipitate was filtered (ADVANTEC, Toyo Roshi Kaisha, Ltd.; pore size = 0.2 mm), washed with water on filter paper, and dried in air at 80°C to constant weight. The relative composition of the clay/surfactant hybrid compounds was determined from the weight gain in the clay and independently confirmed by elemental analysis.[23] The amount of adsorbed Sb(V)TSPP was calculated from the residual amount of Sb(V)TSPP in the filtrate solution. Approximately 60-70% of Sb(V)TSPP was found to cointercalate into the hybrid compounds.

Instrumentation and Methods

The solid surfactant/clay hybrid compound was dispersed in benzene to measure the absorption and emission spectra of the guest porphyrin molecules. The benzene dispersion of the hybrid compound was conducted by addition of dried solid hybrid compound into benzene that is stirred at 23 ± 1°C. For the aggregation experiment, the benzene dispersion continued to stir under 23 ± 1°C and the absorption spectra were measured as a function of time. The benzene dispersion formed a precipitate after standing overnight, but when the resulting dispersion was stirred, stable spectra were observed within one hour, which were reproducible.

The polarized dichroic absorption spectra were measured from cast films of surfactant/clay/Sb(V)TSPP hybrid compound. The cast films were prepared by casting a benzene dispersion of hybrid compound onto a quartz glass plate which was air dried at room temperature. The XRD profiles of surfactant/clay/Sb(V)TSPP cast films from benzene were essentially the same as that for the solid surfactant/clay/Sb(V)TSPP before benzene dispersion indicating that the structure of surfactant/clay hybrid compounds was unaffected by benzene dispersion. The parallel orientation of the hybrid layer against the glass plate was confirmed by observing XRD and SEM images.[25]

The absorption spectra were recorded on UV-2100 (Shimadzu) spectrophotometers. The steady-state emission spectra were obtained on a F-4010 spectrofluorometer (Hitachi). The dichroic absorption spectra were recorded on V-550 spectrophotometers (JASCO) equipped with polarizer units.

A small-angle x-ray scattering (SAXS) instrument was attached to the small-angle x-ray scattering optics (DSC-SRXRD) at the beam-line BL-10C at the Photon Factory (PF), High Energy Accelerator Research Organization (KEK), Tsukuba, Japan. The wavelength of the monochromatic x-rays for DSC-SRXRD was 0.1488 nm whereby the scattered x-rays were detected by a one-dimensional position-sensitive proportional counter (PSPC). The distance between the specimen and the PSPC was 680 nm; that covered 1.25 nm $< S^{-1} = (2 \sin q/l)^{-1} <$ 200 nm, where $2q$ is scattering angle and l is the x-ray wavelength. The sample cell is made of Teflon with a Kapton window for benzene dispersion. The observed intensities were corrected for transmission and subtracted from the intensity of the blank measurement using an empty cell.

Results and Discussion

Cointercalation of Sb(V)TSPP into the Surfactant/Clay Hybrid Layer

An aqueous solution of surfactant and Sb(V)TSPP combines with an aqueous clay dispersion to produce a brown precipitate. Soret absorption maxima in the mixture were 4 nm red-shifted from what is observed in Sb(V)TSPP aqueous solutions, indicating the occurrence of

an intercalation phenomenon of Sb(V)TSPP which will be described in full shortly. Based on the described gravimetric quantification procedure (see Experimental Section), it was found that the brown precipitate was a surfactant/clay/Sb(V)TSPP hybrid compound. The amount of surfactant that was incorporated in addition to the changes in the corresponding layer distances were unaffected by the presence of Sb(V)TSPP.[23-25] This result demonstrated that the Sb(V)TSPP molecules at very light loading levels used in the present work (0.05-0.2 % vs. CEC) do not disturb the structure of the hybrid compound.

It should be noted that the tetra-anionic Sb(V)TSPP molecule was not able to intercalate into cation-exchange-type clays (Sumecton SA) by itself. Sb(V)TSPP could however be readily intercalated in the presence of an ammonium cation-type surfactant. It is suggested that the ammonium surfactant and Sb(V)TSPP form a loosely bound ionic association complex.[22, 34-36, 39] From coulombic arguments, the anionic Sb(V)TSPP is therefore believed to associate and exist in close proximity to the ammonium headgroup of the surfactants and thus be cointercalated.[24, 25, 34, 40]

Swelling Behavior of Polyfluorinated Surfactant/Clay Hybrid Compounds in Benzene

When the polyfluorinated surfactant/clay hybrid compounds are dispersed in benzene, the resultant solution is transparent in the visible region. The spectral transparency is likely a result of the coincident refractive indices between benzene and the clay that has swollen with the hybrid compounds and the solvent. When the benzene dispersion of the hybrid compounds containing Sb(V)TSPP were filtered through a membrane filter made of Teflon (0.2 mm), it was found that there was no measurable absorption from Sb(V)TSPP in the filtrate solution. This result indicates that the Sb(V)TSPP molecules were incorporated into the hybrid compound, even when dispersed in benzene. The fairly good dispersion of the intercalated hybrid compound in benzene suggests good swelling in the solvent.[24, 25] To more fully describe the nature of the structure of the hybrid compound in the benzene dispersion, small-angle x-ray scattering (SAXS) measurements were carried out. One of the principal questions addressed was

whether the hybrid compounds maintained their lamellar structure or not when dispersed in benzene. The SAXS profiles of the C3F-S/clay hybrid compound benzene dispersion and solid film are shown in Figure 2. The sharp *d*(001) peak due to the layered structure was observed for both the solid film and benzene dispersion. This suggests that the C3F-S/clay hybrid compound maintained a layered structure even when dispersed in benzene. The estimated clearance space (distance between the layers) is 3.0 nm for the solid film and 3.8 nm for the benzene dispersion. This expansion of the clearance space clearly demonstrates the penetration of the benzene molecules into the clay layer.

Figure 2. SAXS profiles of C3F-S/clay solid and benzene dispersion.

It is therefore proposed based on the SAXS and spectral absorption data that the bilayer structure is maintained by the incorporation of benzene molecules between each surfactant layer, in a sandwich-type structure.

Aggregation Behavior of Sb(V)TSPP in Polyfluorinated Surfactant/Clay Hybrid Layer

The aqueous mixture of C3F-S/clay/Sb(V)TSPP hybrid compound had a signature Soret maxima that could readily be assigned to the monomer of Sb(V)TSPP (419 nm), but it was relatively red-shifted from what is observed in aqueous solution (415 nm). To further explore the behavior of the porphyrins as a function of environment, a solid film of the aqueous mixture of C3F-S/clay/Sb(V)TSPP was cast by filtering and drying the C3F-S/clay/Sb(V)TSPP aqueous solution (see Experimental Section). The solid film exhibited a more red-shifted Soret absorption maxima at 422 nm. It is known, however, that the Soret absorption maxima of porphyrins are sensitive to solvent polarity. In a less polar solvent, the absorption maxima are shifted toward the red.[41] The large red-shift of Soret band that was observed can be explained by a decrease in the solvent polarity surrounding the Sb(V)TSPP guest molecules through ionic

association formation and intercalation (419 nm)[22, 24, 25] and the severe attenuation of polarity due to vaporization of water molecules in the drying process (422 nm). The aqueous mixture and solid film had Soret maxima that were characteristic of the monomer of Sb(V)TSPP indicating that the Sb(V)TSPP molecules existed as nonaggregated units within the interlayer space, even throughout the mixing with the surfactant/clay, solid film formation, and drying procedures.

Yet, upon dispersion of the dry solid film of C3F-S/Sb(V)TSPP/clay (C3F-S : Sb(V)TSPP = 270 : 0.12% vs. CEC) in benzene, the Soret band of Sb(V)TSPP drastically changed (Figure 3a). During the first 60 min of dispersion, the Soret band exhibited a monomer-like absorbance at 422 nm. For the next 1.5 hours, the 422-nm monomer band diminished and new 388-nm and 438-nm bands were observed with two clean isosbestic points at 393 nm and 431 nm. This spectral change achieved a steady-state distribution after approximately 25 hours. Excitation into the starting 422-nm band provided the monomer fluorescence spectrum at 597 and 652 nm, whereas excitation into the 438-nm envelope gave 602 and 659-nm emission bands, with much lower emission intensities than observed for the monomer. Furthermore, excitation into the 388-nm band gave diminished (or no) emission intensities. These results strongly suggest that the 388-nm and 438-nm absorption bands were associated with different species. The emission quantum yield of porphyrins are recognized to diminish through aggregate formation.[42] These results are consistent with an aggregation phenomenon of the Sb(V)TSPP guest molecules within the interlayer space of the surfactant/clay hybrid compounds. The blue-shifted 388-nm and the red-shifted 438-nm species can be accurately described as dimers of the H-(blue-shifted) and J-type (red-shifted) classes, respectively.[25-27, 30-36, 43] Penetration of benzene molecules into the interlayer is suggested to be a critical step in the formation of the Sb(V)TSPP aggregates.

Figure 3. Absorption spectra of Sb(V)TSPP intercalated in polyfluorinated surfactant/clay hybrid layer. (a) C3F-S, (b) C2F-S, and (c) C1F-S.

The same experiments were carried out for C2F-S and C1F-S polyfluorinated surfactants/Sb(V)TSPP/clay hybrid compounds (C2F-S : Sb(V)TSPP = 160 : 0.12, C1F-S : Sb(V)TSPP = 170 : 0.12% vs. CEC, respectively), and similar absorption spectral changes were observed (Figure 3b, c). Very interestingly, the monomer Sb(V)TSPP absorption remained unchanged after 100 hours of benzene dispersion in the surfactant/clay hybrid compounds containing the hydrocarbon type surfactant C3H-S and CTAB hybrid compounds (C3H-S : Sb(V)TSPP = 170 : 0.12, CTAB : Sb(V)TSPP = 170 : 0.12% vs. CEC, respectively). This latter result clearly indicates that the H- and J-dimerization phenomenon is enhanced in the polyfluorinated environment. The strong lipophobic character of the perfluorinated alkyl chain may act to expel the surrounding hydrophobic Sb(V)TSPP molecules thus causing aggregation. The benzene solvent would then assist in their migration within the interlayer of the hybrid compound through the swelling process and concomitant microcavity generation.

Effect of adsorbed amount of Sb(V)TSPP on aggregation

To more closely examine the aggregation behavior of Sb(V)TSPP, the influence of various adsorbed amounts of Sb(V)TSPP was examined for C3F-S : Sb(V)TSPP = 270 : 0.12 - 0.04% vs. CEC hybrid compounds.[25] The differences in absorption, $DDOD_t$ at two fixed wavelengths λ_1=422 nm (monomer band), λ_2=438 nm (J dimer band) defined in Eq. (1) were plotted against time as shown in Figure 4.

Eq. (1)

Figure 4. Effect of concentration of Sb(V)TSPP on the spectral change.

where $(OD_{li})_{t=0}$ or $_{t=t}$ denotes the observed absorbance for the wavelength λ_i at t=0 or t. The $DDOD_t$ term effectively removes the scattering effect of incident light by the subtraction procedure in Eq. (1). As shown in Figure 4, within the initial first hour, the Sb(V)TSPP

molecules retained their monomer-type absorption character for all adsorbed amounts of Sb(V)TSPP upon dispersion in benzene. The absorption spectral changes commenced after approximately 1.5 hours and stabilized after approximately 25 hours in the benzene dispersion. These results indicate that the time required for penetration of the benzene molecules and subsequent migration of the porphyrins is roughly 1.5 hours.

The Sb(V)TSPP aggregate formation was enhanced by increasing the adsorbed amount of Sb(V)TSPP. Obviously, the absorption spectra were not changed for the sample of Sb(V)TSPP = 0.04% and 0.05% CEC, indicating that no aggregate formation occurred. This suggests that the critical adsorbed amount of Sb(V)TSPP to facilitate aggregate formation is approximately 0.05% of CEC.

The Sumecton SA clay used has all of the properties of a clay mineral. Since it has an area of 1.25 nm^2 per one anion site,[44] when the level of Sb(V)TSPP = 0.05%, the occupational area of one Sb(V)TSPP molecule is estimated to be 2500 nm^2 (= 1.25 nm^2 / 0.0005). This result implies that the area covered in the migration of Sb(V)TSPP molecules is approximately 2500 nm^2. The interlayer of polyfluorinated surfactant/clay may possess a fluid-like character due to the facile penetration of benzene molecules. In contrast, the distance for the migration of Sb(V)TSPP is limited to 2500 nm^2, suggesting that the area of the closed space for the hybrid compound is 2500 $nm.^2$

Kinetics for the aggregation phenomena were obtained through computer simulation analyses. Assuming J-dimer (D_J) and H-dimer (D_H) formation, the kinetics of the two types of dimer formation were expressed by Eq. (2)

$$M + M \rightarrow D_J + D_H \quad (2)$$

where k_1, k_{-1}, and M are the rate constant of formation and dissociation of the dimer porphyrin and monomer, respectively. As shown in Figure 3, both J and H dimers have isosbestic points relative to the monomer porphyrin. This indicates that the formation ratio of J

aggregates and H dimers is constant, as expressed by Eq. (3). The amounts of J and H dimers can be referred to as D; thus, the relations among D_J, D_H, and D are expressed by Eq. (4)

$$[D_J]/[D_H] = A = \text{constant} \quad (3)$$

$$[D_H] + [D_H] = [D] \quad (4)$$

where $[D_J]$, $[D_H]$, and [D] are the concentrations of J dimer, H dimer, and total dimer concentration.

Thus, Eq. (2) was simplified for individual dimer formation as expressed by Eq. (5) and the kinetics of dimer formation are expressed by Eqs. (6) and (7)

$$M + M \rightarrow D \quad (5)$$

$$d[D]/dt = k_1[M]^2 - k_{-1}[D] = d(C_0X)/dt = k_1C_0(1-2X)^2 - C_0k_{-1}X \quad (6)$$

$$X = 1-e^{-pt} \quad (7)$$

where, [M], C_0, $X_{(t)}$ are the concentrations of monomer, initial concentration of Sb(V)TSPP, and molar ratio of the dimer at time = t, respectively. The $DDOD_t$ term in Eq. (1) can be further expressed as Eq. (8), assuming dimer formation.

Eq. (8)

where $De_{(H)}$, $De_{(J)}$, and $De_{(M)}$ denote differences in the absorption coefficients of the H dimer, J dimer, and monomer at l_1 (= 422 nm) and l_2 (= 438 nm). Thus, the first term in Eq. (8) (in brackets), a constant value, can be defined as the b-value. Using the relationships in Eqs. (7) and (8), computer simulated curve fitting for the plots in Fig. 4 were carried out by varying the three parameters k_1, k_{-1}, and b-value. The curves fit very well to the experimental data as shown in Figure 4. The parameters obtained the rate constants k_1, k_{-1}, and b-value and are listed in Table I.

Table I: Rate Constants for Aggregation of Sb(V)TSPP and b-Value

As described previously, aggregation of Sb(V)TSPP was not observed for adsorbed amount of Sb(V)TSPP below 0.05% CEC. Therefore, compared to the sample of the adsorbed Sb(V)TSPP above 0.06% CEC, the obtained rate constants k_1, k_{-1}, and b-value demonstrated fairly good agreement with each other when expressing independent simulations at different adsorbed amounts of Sb(V)TSPP, in which the very small value of k_{-1} showed some fluctuation. The rate of dimerization (k_1) was much slower than that observed for Sn(IV)TSPP (k_1 = 2.58 - 2.52 ′ 10^{-2} $s^{-1}mol^{-1}$).[25] These results clearly indicate that the monomer Sb(V)TSPP effectively dimerized in the polyfluorinated microenvironment.

Surfactant Concentration Effect

The adsorbed amount of polyfluorinated surfactant can be controlled despite the ability of the clay interlayer distance to maintain a constant value (in the case of C3F-S polyfluorinated surfactant, the intercalated levels are from 100 to 440% of the CEC). This suggests that the polyfluorinated surfactant/clay hybrid compounds have given rise to discrete polyfluorinated microcavities.[23] It was previously described that the lipophobic character of perfluorinated environments can expel the Sb(V)TSPP molecules, interrupting their migration within the hybrid interlayer, thus leading to aggregation. It was expected that based on the adsorbed amount of surfactants or more appropriately the volume of the microcavity (excess area) in the interlayer, the aggregation of Sb(V)TSPP would be affected. Aggregation experiments were therefore conducted to test the latter hypothesis by employing various adsorbed amounts of surfactant, while the adsorbed amount of Sb(V)TSPP was fixed at 0.12% CEC. The adsorbed amount of surfactant, occupational area of one surfactant molecule, and excess area in the interlayer is listed in Table II. The "occupational area" is defined as the value of the charge density of the clay (125 $Å^2$ / anionic site)[44] divided by the value of adsorbed amount (number of molecules) of surfactant against CEC.[23] The "excess area" was defined as the value obtained by subtraction of the cross-

sectional area of the most rigidly packed alkyl chain of an ammonium-type surfactant (26 $Å^2$)[23, 45-47] from the observed occupational area of each surfactant.

Table II: Estimation of Adsorbed Amount of Surfactant and Behavior of Sb(V)TSPP

In the case of C2F-S and C3F-S/clay hybrid compounds, clear relationships between adsorbed amounts of polyfluorinated surfactants and aggregation behavior were observed. A control of the adsorbed amounts of surfactant was difficult for C1F-S, C3H-S, and CTAB, mainly because of a saturated adsorption limit of approximately 200% CEC.[23] As described previously, Sb(V)TSPP dimers appear following about 1.5 hour of benzene dispersion and they stabilize after 25 hours in the hybrid compound containing C3F-S = 270% CEC. In the case of the hybrid compound containing C3F-S = 170% CEC, very fast aggregate formation was observed. The Sb(V)TSPP aggregate appeared within 10 minutes of dispersion in benzene and stabilized after 6 hours. However, it was difficult to obtain a reliable estimation of k_1 for C3F-S = 170% CEC due to the very fast aggregate kinetics. For the hybrid compound containing C3F-S = 330% CEC, the monomer Sb(V)TSPP nature remained unchanged even after prolonged standing, in excess of 60 hours. A similar phenomenon was observed for C2F-S/clay hybrid compounds. The Sb(V)TSPP aggregated in the hybrid compound containing C2F-S = 160% CEC. In contrast, the monomer Sb(V)TSPP remained unchanged even after prolonged standing, in excess of 60 hours, in the hybrid compound containing C2F-S = 250% CEC. The Sb(V)TSPP formed an aggregate in the hybrid compounds containing C1F-S = 170% CEC. Again, the monomer Sb(V)TSPP remained unchanged even after prolonged standing, in excess of 60 hours, in the hybrid compound containing hydrocarbon-type surfactants (C3H-S, CTAB = 170% CEC).

Remarkably, Sb(V)TSPP remained as a monomer in the hydrocarbon-type surfactant (C3H-S and CTAB) hybrid compound, even though they have the same or a larger excess area than that found in C1F-S. These results confirm that the polyfluorinated microenvironment in

the interlayer space of the clays is critical to enhancing aggregation of Sb(V)TSPP in which Sb(V)TSPP can be expelled from the polyfluorinated microenvironment.

Influence of Microscopic Orientation of Sb(V)TSPP in Polyfluorinated Surfactant/Clay Hybrid Compounds on Aggregation

Part of this work attempted to more clearly define how certain microcavity constraints affected the guest packing, specifically, with respect to the tilt angle of the porphyrin plane. One of the primary issues of interest in this regard was determining how the metalloporphyrins orient themselves in the interlayer of the clay among the polyfluorinated surfactants. Polarized dichroic absorption measurements[25, 48-51] were carried out for the determination of the molecular tilt angle of Sb(V)TSPP in the hybrid compound. Both the monomer state and aggregated state of Sb(V)TSPP in the hybrid compound from benzene dispersion were cast on quartz glass plates (see Experimental Section).

The relation between the rotation angle (α) of the substrate (or incident angle) and dichroic ratio (R) for uniaxis orientation is expressed as Eq. (9)[52, 53]

Eq. (9)

where, A_y, A_x, q, and g represent the absorption intensities for the vertical and horizontal polarized incident lights, the angle of the molecular axis relative to the optical transition moment, and the tilt angle of the molecule to the substrate normal, respectively. Figure 5 shows the experimental correlation between the α-angle and the dichroic ratio (R) of the monomer Sb(V)TSPP in the interlayer space of a C3F-S/clay hybrid cast film (C3F-S : Sb(V)TSPP = 270 : 0.12% CEC) measured at the Soret monomer absorption maxima (422 nm).

Figure 5. α dependence of dichroism ratio (R) of Sb(V)TSPP/C3F-S/SA cast film.

The R value depends on the α-angle and had a maximum at α = 0°. This indicates that the Sb(V)TSPP molecules are oriented not only in the clay but also subsequently on the glass plate, since the hybrid clay particles are aligned in the film. The Soret absorption of Sb(V)TSPP arises from the π-electron conjugation in the porphyrin plane; thus, the optical transition moment of Soret absorption exists in the plane of the porphyrin ring. The molecular axis of Sb(V)TSPP is defined as a normal line in the porphyrin plane and the angle (q) of the molecular axis to the optical transition moment is estimated to be 90° (Figure 6). By fitting Eq. (9) to the correlation between R, α, and q, the tilt angle (g) of Sb(V)TSPP could be estimated. The solid line in Figure 5 is the fitting result based on Eq. (9). It can be seen that the experimental data were well fitted by Eq. (9), and tilt angle of Sb(V)TSPP was estimated as g=45.7°. Thus, the monomer Sb(V)TSPP orients itself 45.7° relative to the clay layer (the same experiment was carried out for the H dimer (analyzed at 388 nm) and the J dimer (analyzed at 438 nm) of Sb(V)TSPP in C3F-S /clay hybrid compounds). (The dipole moments of the H and J dimers are tilted 47.0 and 44.9 ° versus the clay layer, respectively.)

Figure 6. Optical transition moment of porphyrin Soret band.

Based on the x-ray analysis, the C3F-S molecules might orient themselves approximately 35° relative to the clay layer.[23] The tilt angles of Sb(V)TSPP are different from those of the C3F-S polyfluorinated surfactant, suggesting that the orientation of the Sb(V)TSPP molecules are independent of the orientation of the C3F-S molecules. It is thought that the Sb(V)TSPP molecules are located outside of the oriented C3F-S polyfluorinated surfactant assemblies and weakly associated with the ammonium cation of C3F-S. The benzene solvent, thus, could easily transport Sb(V)TSPP molecules for aggregation.

The Sb(V)TSPP molecules can orient themselves in nonparallel orientations versus the clay surface and may thus be able to induce the two types of dimer (H and J) formation as described previously in which the clearance space of the hybrid compounds is estimated to be about 30 Å.[23] Yet this clearance distance can sufficiently accommodate the Sb(V)TSPP molecule

(diagonal direction of SO^{3-} to SO^{3-} of Sb(V)TSPP is ca. 20 Å). It might be that the degrees of translational freedom of Sb(V)TSPP in the normal direction of the clay layer are relatively high. Thus, two types of dimers can be formed simultaneously. One includes a stacked orientation of the two porphyrin rings (strongly p conjugated H dimer), while the other is described as two porphyrin rings oriented in a staggered structure (weakly p conjugated J dimer). The proposed dimerization mechanisms of Sb(V)TSPP in polyfluorinated surfactant/clay interlayer are shown in Figure 7.

Figure 7. Proposed schematic drawing of aggregation mechanism of Sb(V)TSPP in the polyfluorinated surfactant/clay interlayer.

In contrast, it was found that Ge(IV)TSPP molecules orient themselves 30.3° against the clay surface with no concomitant dimer formation for Ge(IV)TSPP having the same tilt angle of C3F-S; apparently, the Ge(IV)TSPP is deeply trapped within the surfactant assemblies in the interlayer of the clay. In contrast, Sn(IV)TSPP molecules orient themselves 11.7° against the clay surface (almost parallel to the clay surface), but selective H-dimer formation for Sn(IV)TSPP was observed.[25] It is noteworthy that metalloporphyrins with different centered metal atoms induce different aggregation constructs and have different orientational structures in the interlayer space. But it is not yet clear why the different metalloporphyrins induce different distribution and aggregation behavior; this will require further study.

Summary (Aggregation Mechanism)

The spontaneous aggregation phenomena of Sb(V)TSPP that are intercalated in polyfluorinated surfactant/clay hybrid compounds was investigated. The aggregation behavior was observed only by employing polyfluorinated-type surfactants. Two types of dimers such as H and J dimers were observed simultaneously. The clear enhancement of aggregation was observed by increasing the adsorbed amount of Sb(V)TSPP, and computer curve fitting

assuming dimer formation provided a good fit to experimental results. The aggregation was inhibited by increasing the adsorbed amount of surfactant or decreasing the excess area. Dichroic absorption spectra measurements revealed that the Sb(V)TSPP molecules in the interlayer of C3F-S/clay hybrid compound orient themselves 45.7° versus the clay layer.

Based on the these results, it has been proposed that the aggregation mechanisms of Sb(V)TSPP in polyfluorinated surfactant/clay interlayer are as follows: (I) Sb(V)TSPP in surfactant/clay hybrid exists as a monomer state, prior to benzene dispersion (Figure 7a); (II) whereupon there is swelling and an increase in fluidity of the interlayer with penetration of benzene molecules (Figure 7b); (III) rejection of Sb(V)TSPP from the polyfluorinated environment and migration to the excess space in hybrid layer in which the limited migration area of Sb(V)TSPP is estimated to be over a 2500 nm^2 area; and (IV) H- and J-types of Sb(V)TSPP dimer formation occur in the excess area (polyfluorinated microcavity) of the hybrid compound (Figure 7c).

Upon benzene dispersion, the Sb(V)TSPP form two types of dimer such as the H and J dimer simultaneously within the polyfluorinated surfactant/clay hybrid layer. The Sn(IV)TSPP forms only the H dimer in the polyfluorinated surfactant/clay hybrid compound, whereas Ge(IV)TSPP remains as a monomer in polyfluorinated surfactant/clay hybrid compounds.[25] It is not yet clear why the metalloporphyrins within the interlayer of clay behave differently as a function of central metal atoms. The systematic examination of other metalloporphyrins with different metal atoms, formal charges, axial ligands, and structures *(meso*-phenyl groups, etc.) may reveal more details of the aggregation mechanism of different metal-centered porphyrins in polyfluorinated microenvironments.

Acknowledgements

LAL acknowledges partial funding for this work by the member companies of IPST. Parts of this work will fulfill the Ph.D. requirements of YT.

References and Notes

[1] Grim, R. E. *Clay Mineralogy*; McGraw-Hill: New York, 1953.

[2] Theng, B. K. *The Chemistry of Clay-Organic Reactions*; Adam Hilger: London, 1974.

[3] Van Olphen, H. *An Introduction to Clay Colloid Chemistry*, 2nd ed.; Wiley-Interscience: New York, 1977.

[4] Shiramizu, H. *Clay Mineralogy*; Asakura-shoten: Tokyo, 1988.

[5] Sposito, G.; Prost, R. *Chem. Rev.* **1982**, *82*, 553.

[6] *Intercalation Chemistry*; Whittingham, M. S.; Jacobson, A. J., Eds.; Academic Press: New York, 1982.

[7] Ogawa, M.; Kuroda, K. *Chem. Rev.* **1995**, *95*, 399.

[8] Takagi, K.; Shichi, T. In *Photophysics and Photochemistry in Clay Minerals in Solid State and Surface Photochemistry*; Ramamurthy, V., Schanze, K. S., Eds.; Marcel Dekker: New York, 2000; Vol. 5, p. 31.

[9] Shichi T.; Takagi K. *J. Photochem. Photobiol. C: Photochem. Rev.* **2000**, *1*, 113.

[10] Lagaly, G. *Clay Minerals* **1981**, *16*, 1.

[11] Lagaly, G. *Clay Minerals* **1982**, *30*, 215.

[12] Weiss, A. *Chem. Ber.* **1958**, *91*, 487.

[13] Weiss, A. *Angew. Chem.* **1963**, *75*, 113.

[14] Weiss, A. *Angew. Chem. Int. Ed. Engl.* **1963**, *2*, 134.

[15] Okahata, Y.; Shimazu, A. *Langmuir* **1989**, *5*, 954.

[16] Vaia, R. A.; Teukolsky, R. K.; Giannelis, E. P. *Chem. Mater.* **1994**, *6*, 1017.

[17] Xu, S.; Boyd, S. A. *Langmuir* **1995**, *11*, 2508.

[18] Banks, R. E. *Organofluorine Chemicals and their Industrial Applications*; Ellis Horwood Ltd.: Chichester, U. K., 1979.

[19] Negishi, A. *Chemistry of Fluorine*; Maruzen: Tokyo, 1988.

[20] Kitazumi, T.; Ishihara, T.; Taguchi, T. *Chemistry of Fluorine*: Kodansha Scientific: Tokyo, 1993.

[21] Lawson, C. W.; Hirayama, F.; Lipsky, S. J. Chem. Phys. **1969**, *51*, 1590.

[22] Kameo, Y.; Takahashi, S.; Kowald, M. K-.; Ohmachi, T.; Takagi, S.; Inoue, H. *J. Phys. Chem. B* **1999**, *103*, 9562.

[23] Yui, T.; Yoshida, H.; Tachibana, H.; Tryk, D. A.; Inoue, H. *Langmuir*, in press.

R.B. intercalation

[24] Yui, T.; Uppili, S. R.; Shimada, T.; Tryk, D. A.; Yoshida, H.; Inoue, H. *Langmuir*, submitted.

[25] Matsuoka, R.; Yui, T.; Sasai, R.; Takagi, K.; Inoue, H. *Mol. Cryst. and Liq. Cryst.* **2000**, *341*, 333.

[26] *The Porphyrin Handbook*; Kadish, K. M., Smith, K. M., Guilard, R., Eds.; Academic Press: New York, 1999.

[27] Takagi, S.; Inoue, H. In *Molecular and Supramolecular Photochemistry of Porphyrins and Metalloporphyrins in Clay Minerals in Solid State and Surface Photochemistry*; Ramamurthy, V., Schanze, K. S., Eds.; Marcel Dekker: New York, 2000; Vol. 6; p. 215.

[28] Shiragami, T.; Kubomura, K.; Ishibashi, D.; Inoue, H. *J. Am. Chem. Soc.* **1996**, *118*, 6311.

[29] Takagi, S.; Suzuki, M.; Shiragami, T.; Inoue, H. *J. Am. Chem. Soc.* **1997**, *119*, 8712.

[30] Yamashita, K.; Kihara, N.; Shimidzu, H.; Suzuki, H. *Phochem. Photobiol.* **1982**, *35*, 1.

[31] Jones, R.; Tredgold, R. H.; Hoorfar, A. *Thin Solid Films* **1985**, *123*, 307.

[32] Beswick, R. B.; Pitt, C. W. *Chem. Phys. Lett.* **1988**, *143*, 589.

[33] Schick, G. A.; Schreiman, I. C.; Wagner, R.W.; Lindsey, J. S.; Bocian, D. F. *J. Am. Chem. Soc.* **1989**, *111*, 1344.

[34] Khairutdinov, R. F.; Serpone, N. *J. Phys. Chem. B* **1999**, *103*, 761.

[35] Maiti, N. C.; Mazumdar, S.; Periasamy, N. *J. Phys. Chem. B* **1998**, *102*, 1528.

[36] Hinoue, T.; Kobayashi, J.; Ozeki, T.; Watarai, H. *Chem. Lett.* **1997**, 763.

[37] Usami, H.; Takagi, K; Sawaki, Y. *J. Chem. Soc. Perkin.Trans. 2.* **1990**, 1723.

[38] Takagi, S.; Shimada, T.; Yui, T.; Inoue, H. *Chem. Lett.* **2001**, 128.

[39] Bilski, P.; Dabestani, R.; Chignell, C. F. *J. Phys. Chem.* **1991**, *95*, 5784.

[40] Yamaguchi, Y.; Yui, T.; Takagi, S.; Shimada, T.; Inoue, H. *Chem. Lett.* **2001**, 644.

[41] Relationship between solvent polarity and Soret absorption maxima of Sb(V)TSPP is as follows: H_2O (γ: 78.4; 415.2 nm), H_2O : methanol = 2 : 1 vol. / vol. (γ: 62.9; 416.4 nm), H_2O : methanol = 1 : 1 vol. / vol. (γ: 55.0; 417.5 nm), H_2O : methanol = 1 : 2 vol. / vol. (γ: 47.2; 418.0 nm), methanol (γ: 32.7; 418.6 nm), ethanol (γ: 24.6; 420.2 nm), cyclohexanone (γ: 18.3; 421.2 nm) pyridine (γ: 12.0 ; 429 nm)

[42] Ghosh, P.K; Bard, A.J. *J. Phys. Chem.* **1984,** *88,* 5519.

[43] Fidder, H.; Terpstra, J.; Wiersma, D.A. *J. Chem. Phys.* **1991**, *94*, 6895.

[44] Calculated from the values of the surface area of the Sumceton SA (750 $m^2\ g^{-1}$) and CEC (0.998 meqv g^{-1} / g): 750 $m^2\ g^{-1}$ / (0.998 meqv g^{-1} ' N_A) = 1.25 $nm^2\ eqv^{-1}$, where N_A is Avogadro's number.

[45] Li, B.; Fujii, M.; Fukuda, K.; Kato, T.; Seimiya, T. *J. Colloid Interface Soc.* **1999**, *209*, 25.

[46] Fujii, M.; Li, B.; Fukuda, K.; Kato, T.; Seimiya, T. *Langmuir* **2001**, *17*, 1138.

[47] Tsao, Y.-H.; Yang, S. X.; Evans, D. F. *Langmuir* **1991**, *10*, 3154.

[48] Sasai, R.; Shin'ya, N.; Shichi, T.; Takagi. K.; Gekko, K. *Langmuir* **1999**, *15*, 413.

[49] Sonobe, K.; Kikuta, K.; Takagi, K. *Chem. Mater.* **1999**, *11*, 1089.

[50] Sasai, R.; Shichi, T.; Gekko, K.; Takagi, K. *Bull. Chem. Soc. Jpn.* **2000**, *73*, 1925.

[51] Sasai R.; Itoh, H.; Shindachi, I,; Shichi, T.; Takagi, K. *Chem. Mater.* **2001**, *13*, 2012.

[52] Michl, J.; Thulstrup, E. W. *Spectroscopy with Polarized Light*; VHC: New York, 1986; p. 75.

[53] Fukuda, K.: Kato, T.; Nakahara, H.; Shibasaki, Y. *Chohakumakubunsi Soshikimaku-no Kagaku*; Koudansha: Tokyo, 1993; p. 89.

Figure Captions

Figure 1. Schematic structure of C3F-S/clay hybrid compounds for various amounts of adsorbed C3F-S molecules: (a) amount approximately equal to CEC; (b) amount in excess of CEC; and (c) 440% CEC. Under the conditions depicted in (a) or (b), the polyfluorinated

surfactant/clay hybrid compounds have molecular dimension microcavities in the interlayer. The intercalation levels of surfactant control the size of the microcavity.

Figure 2. The small-angle x-ray scattering profiles of C3F-S/clay hybrid compounds (C3F-S = 270% CEC): (a) dry film and (b) benzene dispersion.

Figure 3. Absorption spectral changes of Sb(V)TSPP cointercalated in the polyfluorinated surfactant/clay hybrid compounds upon benzene dispersion: (a) C3F-S : Sb(V)TSPP = 270 : 0.12% CEC; (b) C2F-S : Sb(V)TSPP = 160 : 0.12% CEC; and (c) C1F-S : Sb(V)TSPP = 170 : 0.12% CEC hybrid compounds.

Figure 4. Effects of adsorbed amount of Sb(V)TSPP on the spectral changes in C3F-S (270% CEC)/clay hybrid compounds. Analyzed at 8_1 = 422 nm, 8_2 = 438 nm. Adsorbed amount of Sb(V)TSPP were (?) 0.12; (?) 0.08; (?) 0.06; (?) 0.05; and (?) 0.04% CEC.

Figure 5. The experimental relationship between dichroism ratios (R) and ∀-angle of the C3F-S : Sb(V)TSPP = 270 : 0.12%/clay hybrid cast film at Soret monomer absorption band (422 nm) and solid line of the calculated curve from Eq. 9.

Figure 6. Schematic orientation of transition moment and molecular axis in porphyrin molecule. The Soret absorption is caused by this transition moment. The transition moment exists in the plane of the porphyrin ring.

Figure 7. Schematic drawing for the aggregation mechanisms of Sb(V)TSPP in polyfluorinated surfactant/clay hybrid compounds: (a) solid state; (b) swollen in benzene, the clay layer expands due to incorporation of benzene molecules; and (c) migration of Sb(V)TSPP molecules into the interlayer with subsequent dimer formation.

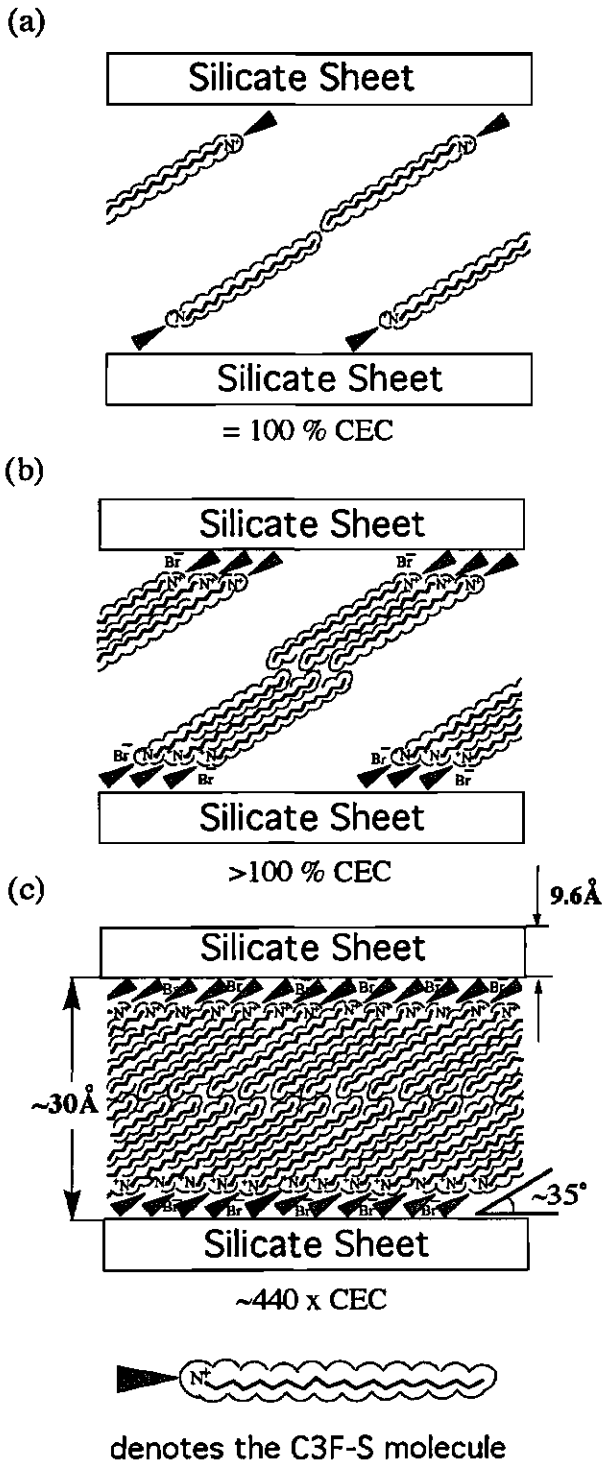
(a)
Silicate Sheet
Silicate Sheet
= 100 % CEC
(b)
Silicate Sheet
Silicate Sheet
>100 % CEC
(c)
9.6Å
Silicate Sheet
~30Å
~35°
Silicate Sheet
~440 x CEC
denotes the C3F-S molecule

Figure 1.

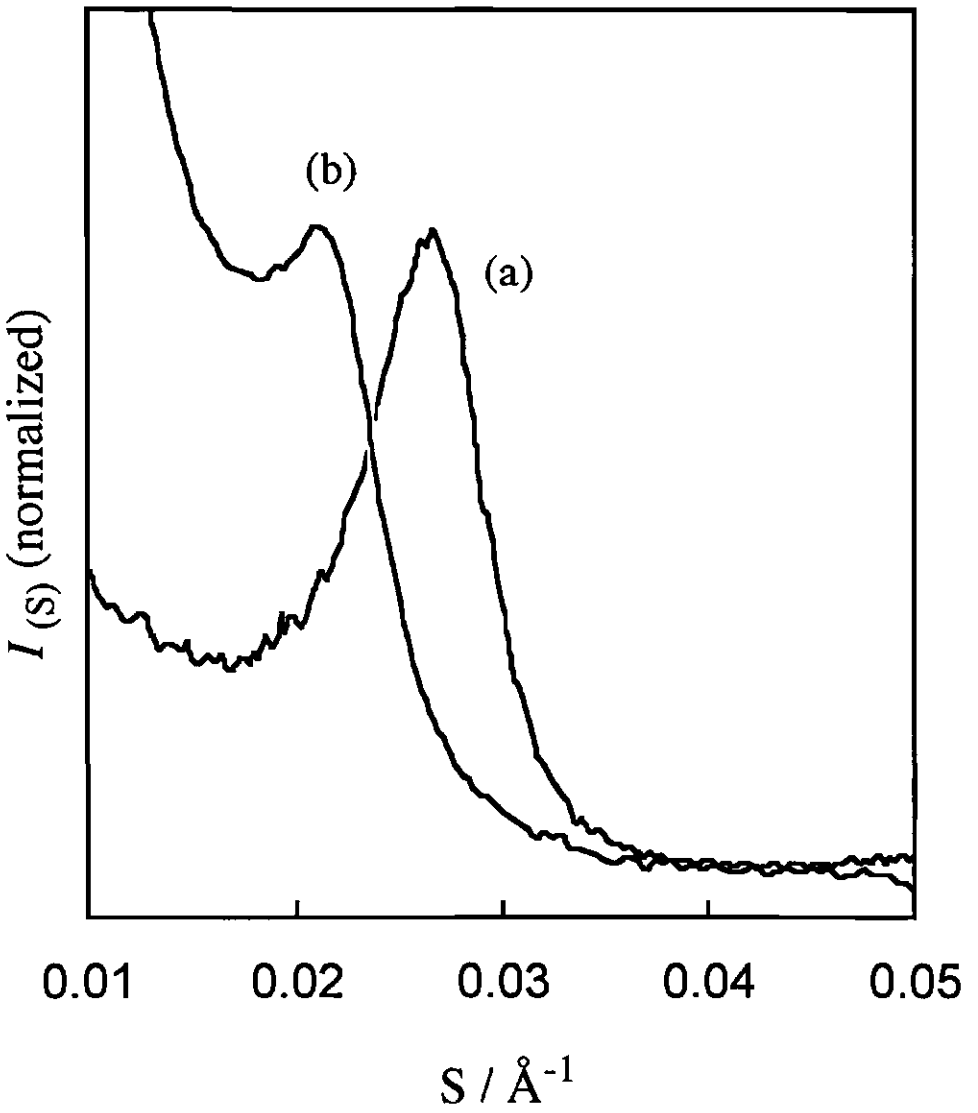

Figure 2.

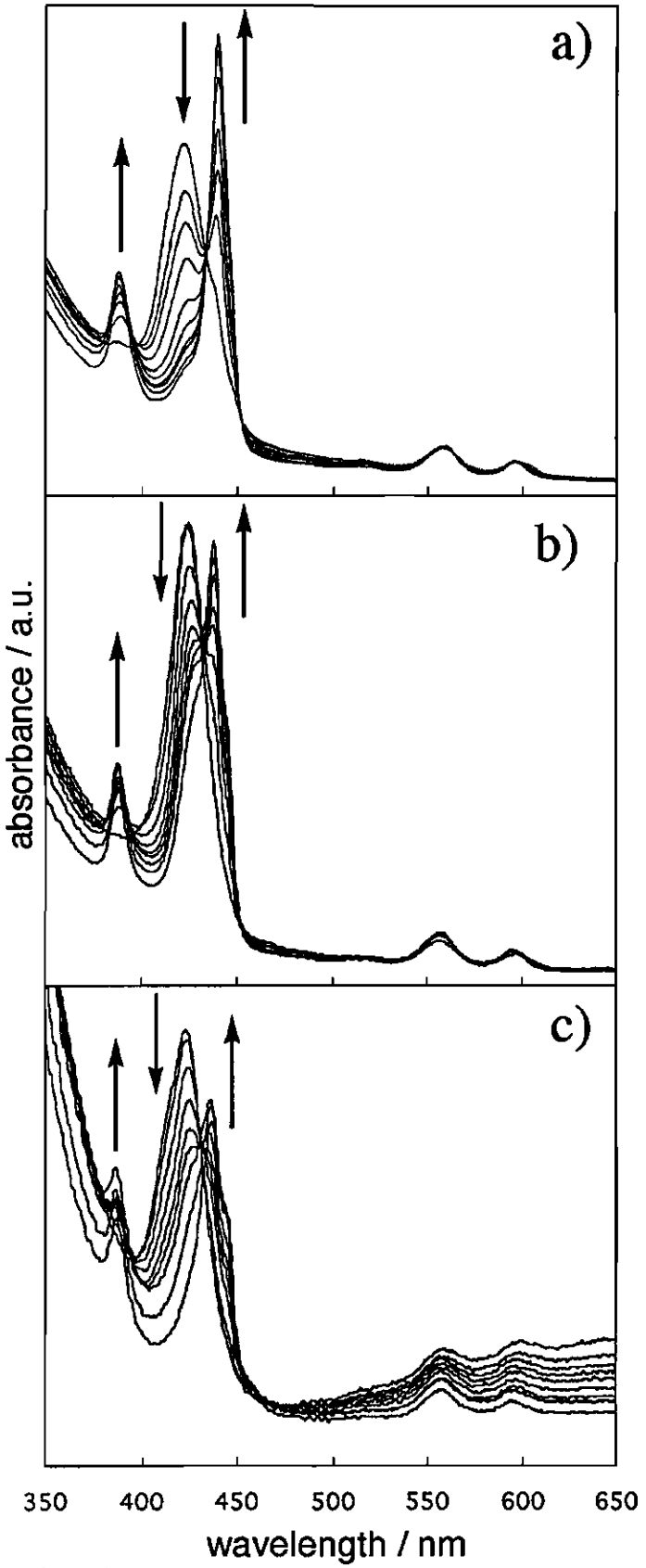

Fig.3

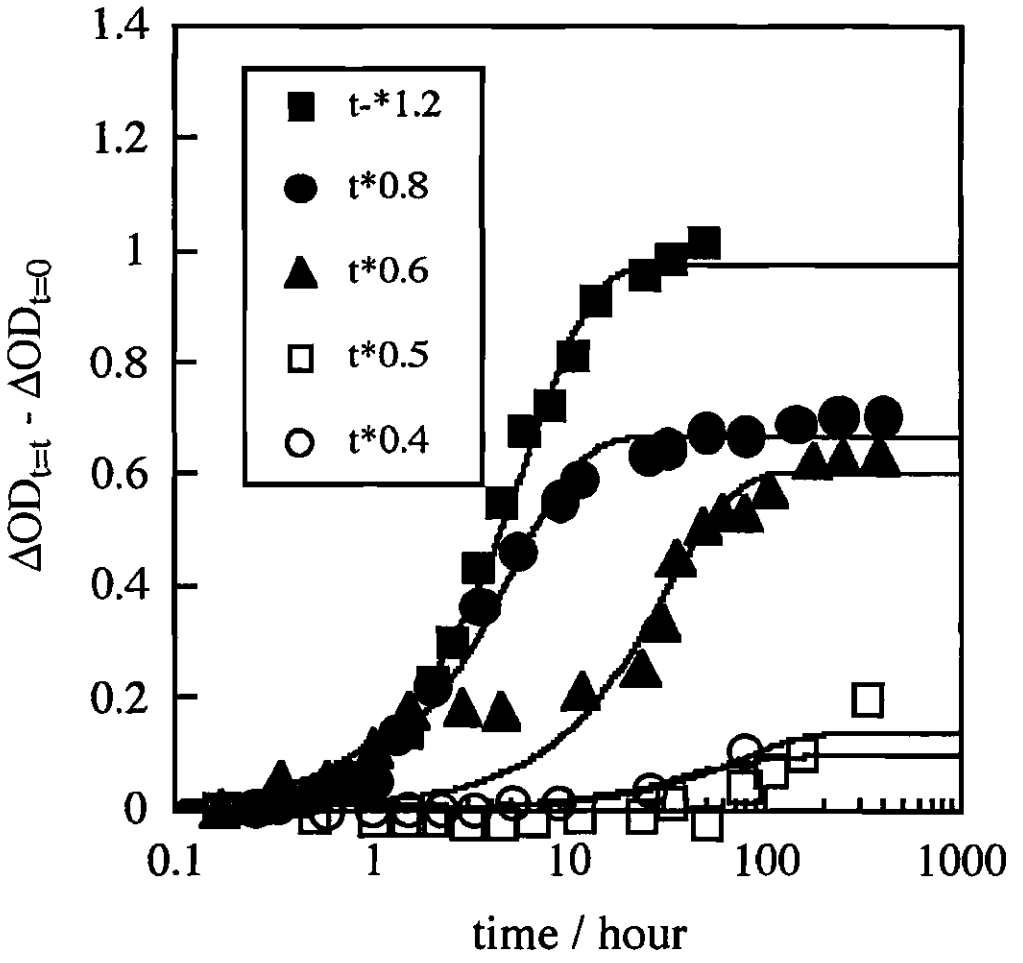
1.4
1.2
1
0.8
0.6
0.4
0.2
0
0.1
1
10
100
1000
t-*1.2
t*0.8
t*0.6
t*0.5
t*0.4
ΔODt=t - ΔODt=0
time / hour

Fig. 4

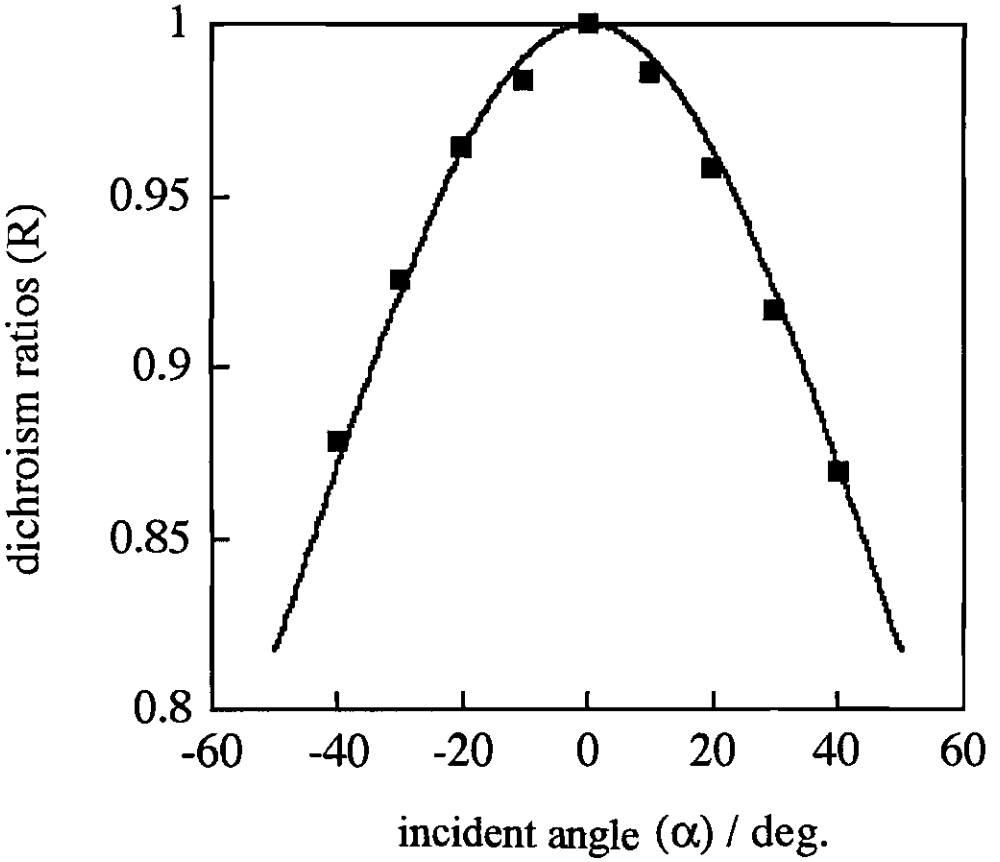
1
0.95
0.9
0.85
0.8
dichroism ratios (R)
-60
-40
-20
0
20
40
60
incident angle (α) / deg.

Fig. 5

Scheme

CnF-S surfactant

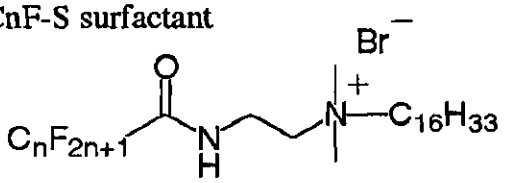

n=1: C1F-S n=2: C2F-S n=3: C3F-S

C3H-S surfactant

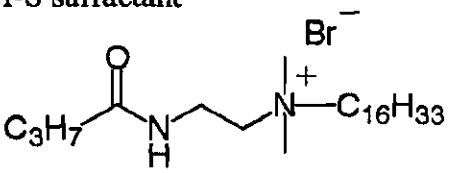

Sb(V)TSPP

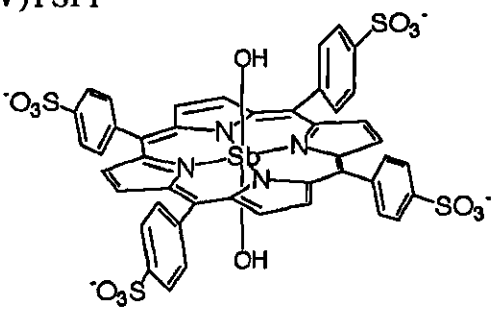

Table 1:

adsorbed amount	$C_0 \times 10^{-8}$	$b \times 10^{7}$	$k_1 \times 10^{-1}$	$k_{-1} \times 10^{-22}$
% CEC	mol dm^{-2}	M^{-1} cm^{-1}	s dm^2 mol^{-1}	s
0.12	16.0	1.22	2.00	9.99
0.08	10.6	1.25	2.04	2.29
0.06	8.0	1.51	1.57	16.49
0.05	6.6	0.29	1.57	16.47
0.04	5.3	0.53	1.42	21.33

Table 2: Relationship Between Adsorbed Amount of Surfactant and Aggregate Formation of SbTSPP[a] in Interlayer Space.

surfactant	adsorbed amount of surfactant	occupational area	excess area	aggregate formation
	% CEC	Å^2	Å^2	
C3F-S	330	37	11	no
	270	45	19	yes
	170	71	45	yes (very fast)
C2F-S	250	50	24	no
	160	75	49	yes
C1F-S	170	74	48	yes
C3H-S	170	73	47	no
CTAB	170	79	53	no

[a] Adsorbed amount of Sb(V)TSPP is 0.12 % CEC.

Equations (1) - (6)

$$\Delta\Delta OD_t = (\Delta OD_{\lambda 1} - \Delta OD_{\lambda 2})_{t=0} - (\Delta OD_{\lambda 1} - \Delta OD_{\lambda 2})_{t=t} \quad (1)$$

$$M + M \underset{k_{-1}}{\overset{k_1}{\rightleftharpoons}} D_J + D_H \quad (2)$$

$$A = [D_J] / [D_H] = \text{constant} \quad (3)$$

$$[D_J] + [D_H] = [D] \quad (4)$$

$$M + M \underset{k_{-1}}{\overset{k_1}{\rightleftharpoons}} D \quad (5)$$

$$\frac{d[D]}{dt} = k_1[M]^2 - k_{-1}[D]$$

$$= \frac{d(C_0X_{(t)})}{dt} = k_1C_0^2(1 - 2X_{(t)})^2 - k_{-1}C_0X_{(t)} \quad (6)$$

Equations (7) - (9)

$$X_{(t)} = \frac{1 - e^{-pt}}{(1/n) - (1/m)e^{-pt}}$$

$$\left(m = \frac{\eta - \sqrt{\eta^2 - 16}}{8}, \quad n = \frac{\eta + \sqrt{\eta^2 - 16}}{8}, \quad p = \frac{4k_1C_0}{\sqrt{\eta^2 - 16}}, \quad \eta = 4 + \frac{k_{-1}}{k_1C_0} \right) \tag{7}$$

$$\begin{aligned} &\Delta OD_{t=t} - \Delta OD_{t=0} \\ &= [(\frac{1}{1+A})\,(A\,\Delta\varepsilon_{(H)} + \Delta\varepsilon_{(J)}) - 2\Delta\varepsilon_{(M)}]\,C_0\,X_{(t)} \\ &= b\,C_0\,X_{(t)} \end{aligned} \tag{8}$$

$$\begin{aligned} R &= A_y / A_x \\ &= \{2[\sin^2\theta + \sin^2\alpha(3\cos^2\theta - 1)] - \\ &\quad (3\cos^2\theta - 1)(3\cos^2\theta - 1)\sin^2\gamma\} / \{2\sin^2\theta + \\ &\quad (2 - 3\sin^2\theta)\sin^2\gamma\} \end{aligned} \tag{9}$$

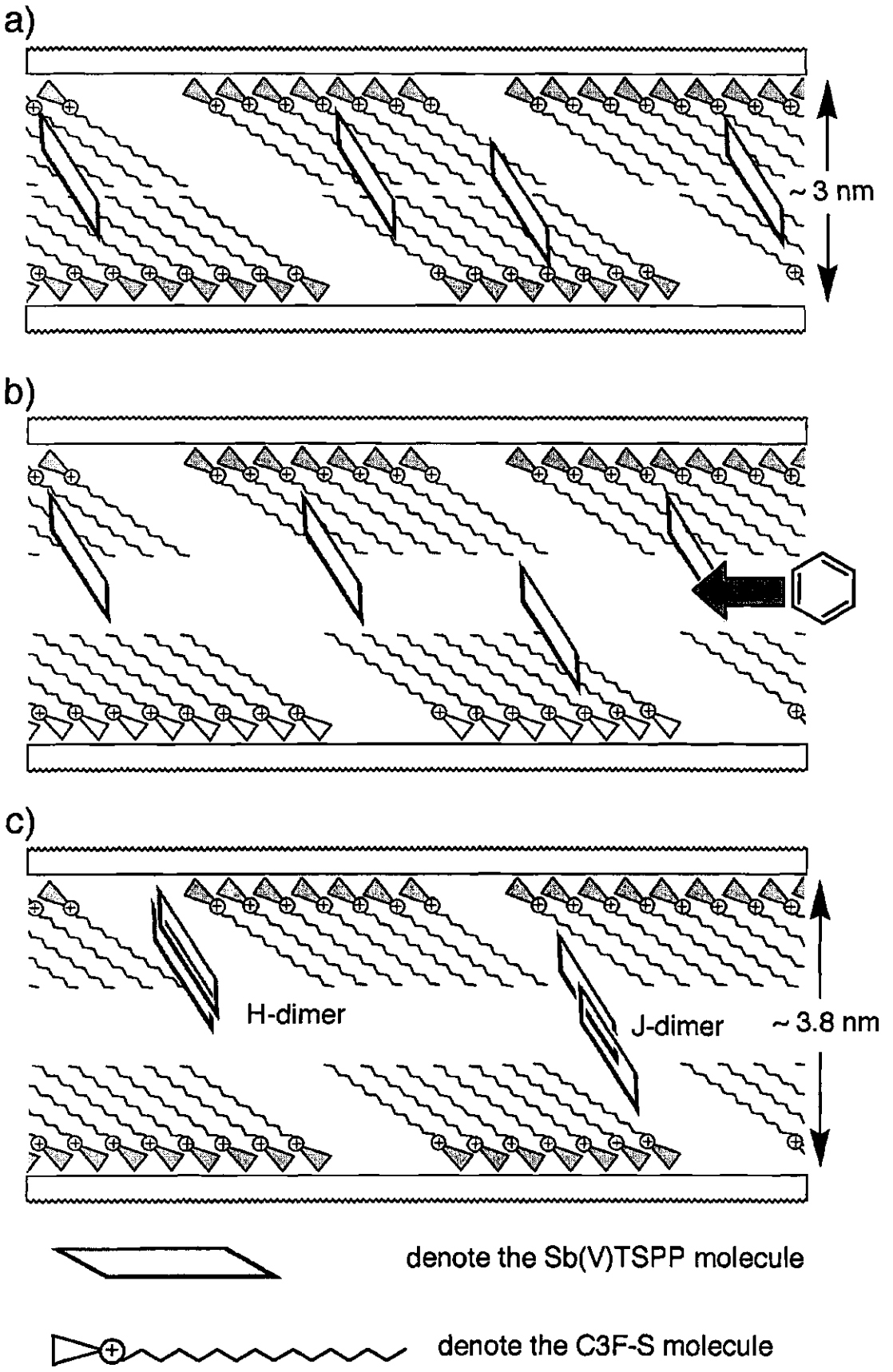
a)
~ 3 nm
b)
c)
H-dimer
J-dimer
~ 3.8 nm
denote the Sb(V)TSPP molecule
denote the C3F-S molecule

Fig. 7